Journal of Engineering and Computer Sciences
Qassim University, Vol. 11, No. 1, pp. 57-78 (January 2018/Rabi II 1439H)

Control of Double-Fed Wind-Driven Induction Generator for Catching the Maximum Mechanical Power

Ayman M. Abdalsamie[1] Adel Shaltout[2]

[1]Giza Systems T&D, New Cairo, Cairo, Egypt
[2] Power and Machines Dept., College of Engineering, Cairo Univ., Giza, Egypt

Aymanabdalsamie@gmail.com

ABSTRACT. Nowadays, Exploitation of the renewal wind energy such as wind energy finds increasing interest. Wind-turbines prime movers operate at variable speed. Therefore, it is recommended to use induction generators with such prime movers as it is suitable for such conditions. The present research is aimed at improving the performance of a wind-driven double-fed induction generator (DFIG) system at different wind speeds. A set of two converters in the rotor circuit has been controlled to inject a certain voltage. This voltage enables the generator to run at the speed which allows the wind turbine to extract the maximum power from the wind. The research presents a new analytical technique for calculating the injected voltage and power necessary to catch the maximum wind power. The induction generator has been modelled at steady-state conditions using frequency domain equivalent circuit. Computer-programs have been designed to compute the performance characteristics of the DFIG with this basic control strategy and compare it to the uncontrolled generator. The comparison has revealed that the performance of the controlled DFIG is clearly improved.

Keywords: Wind-driven, generator, voltage, power, circuit, control strategy

1. Introduction

The utilization of wind energy is very important and finds nowadays great interest. This interest has become vital as many energy experts have expected the rapid exhaust of the conventional energy resources. Therefore, generation of the electrical power from the sustainable energy resources such as wind energy has become on the top of the solution priorities.

Wind-turbines have the problem of being of variable and unexpected speeds. The frequency of the generated voltage of synchronous generators is directly proportional to the prime mover speed. Therefore, to have a fixed frequency, other generator types or unconventional solutions should be used. Use of induction generators is a good practical solution [1, 2].

Because the wind has variable speed character, the performance of the wind driven induction generator will clearly differ depending on the wind speed. Therefore, it is necessary to control the generator to ensure getting a good performance at all wind speeds. Amelioration of the performance of the grid-connected induction generators at different wind speeds has been achieved through the use of converters in the stator side for single-fed generators [3-11], or through the use of a rectifier-inverter set in the rotor side for double fed generators [12-17].

Many researchers investigated the performance of the doubly-fed induction generators. Carlos [12] suggested a technique by which the current of the grid-connected induction generator is controlled while driven by a variable-speed wind-turbine. Holdworth et. al. [13] have carried out a comparison between fixed-speed induction-generators (FSIG) and variable speed doubly-fed induction generators (DFIG). They showed that the FSIG during short circuits induces voltage sags at the terminal busbars which may lead eventually to voltage instability, while the DFIG improves the terminal bus voltage profiles thus increasing the stability margins. Fernandez et. al. [14] have developed a new way of aggregation of DFIGs under different incoming winds by an equivalent wind turbine to approximate the active and reactive powers of wind farms with high number of wind turbines. De Almeida and Lopes [15] have described a control approach to integrate a frequency regulation capability into a DFIG active power control loop using the frequency deviation. Such an approach could contribute to increase the system robustness, reducing frequency changes following disturbances. Shaltout, et. al, [16] proposed a simple control strategy of DFIG to facilitate harnessing maximum power extracted from the wind. This strategy is based on controlling the slip power, which is drawn from the rotor circuit and fed to the power grid through a rectifier-inverter set. Abdel-halim, et. al [17] presented a stator and rotor combined control method for induction generators to trace the maximum wind power and at the same time the power factor is adjusted at unity. The optimization technique is based on an approximate circuit model which neglects the iron losses and fixes the magnetizing current.

The present paper aims at improving the performance of the wind-driven double-fed induction generator (DFIG) at the different wind speeds employing a basic control technique from the rotor side. The control is employed through injecting a voltage in the rotor side in-phase or in-phase opposition to the rotor current using a rectifier-inverter set, and controlling the voltage magnitude such that the generator will trace the maximum wind power point. This technique will ensure catching the maximum wind mechanical power, and at the same time minimizing the apparent power dealt with through the rotor slip rings. In the present research a developed method is presented for calculating the required injected voltage at the different wind speeds. The research is performed through developing a steady-state frequency domain circuit model for the generator and a conventional mathematical model for the rest of the system. Based on these models, computer programs will be developed to compute the performance characteristics of the DFIG. Thereafter, the performance will be compared to that of the uncontrolled IG.

2. System Description and Control Strategy

2.1. Studied System

The system under study (Figure (1)) comprises a variable-speed wind-driven grid-connected double-fed induction generator. The stator of the generator is directly connected to the grid. The generator slip-ring rotor is connected to the grid through a set of two controlled three-phase bridge converters.

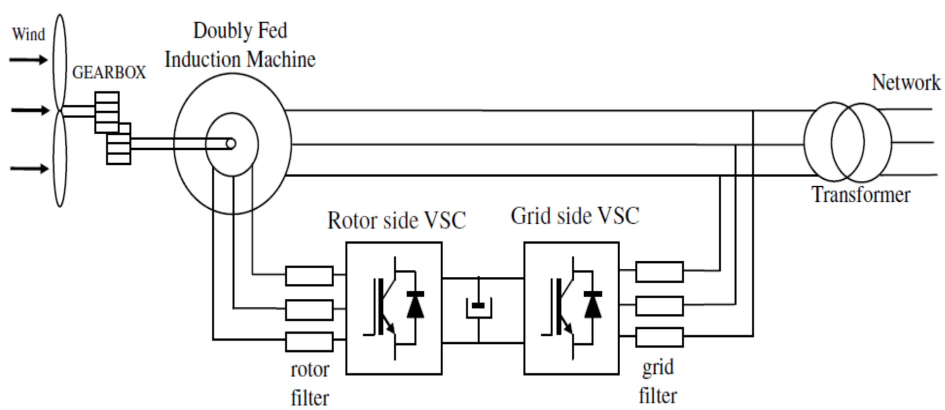

Fig. (1). DFIG system

2.2. Control Strategy

The generator control is performed by adjusting the magnitude of the rotor injected voltage while its phase is in-phase or in-phase opposition to the rotor current. The control strategy aims to regulate the speed of the generator to force the turbine to operate such that it will [18],

i. Limit the minimum speed of operation (region 1) at low wind speeds.
ii. Follow the curve of maximum power extraction from variable speed operation with partial load (region 2) at intermediate wind speeds.
iii. Limit the maximum speed at partial load operation up to the rated generator power (region 3) at high wind speeds.

3. System Modelling

3.1. Wind-turbine Modelling

Commonly, the torque and power are expressed in terms of non-dimensional torque and power coefficients (C_Q) and (C_P) respectively as follows [18& 19]

$$T_r = \frac{1}{2}\rho\pi R^3 C_Q(\lambda, \beta) V^2, \quad (1)$$

$$P_r = C_P(\lambda, \beta) P_V = \frac{1}{2}\rho\pi R^2 C_P(\lambda, \beta) V^3, \quad (2)$$

Note that the coefficients are written in terms of the pitch angle β and the so-called tip-speed-ratio λ defined as

$$\lambda = \frac{\Omega_r R}{V}. \quad (3)$$

Figure (2) depicts typical coefficients $C_Q(\lambda)$ and $C_P(\lambda)$ of fixed pitch turbines in two-dimensional graphs.

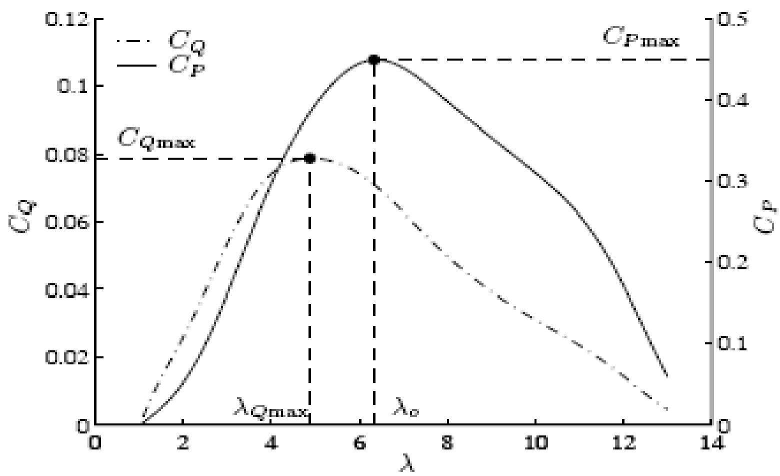

Fig. (2). Typical variations of C_Q and C_P for a fixed-pitch wind turbine

3.1. Single-Fed Induction Generator Modelling

Figure (3) shows the steady state equivalent circuit of the normally run induction generator with its stator terminals connected to the supply, and its rotor is short-circuited. This is the usual equivalent circuit of induction machines [2] keeping in mind that the slip is negative.

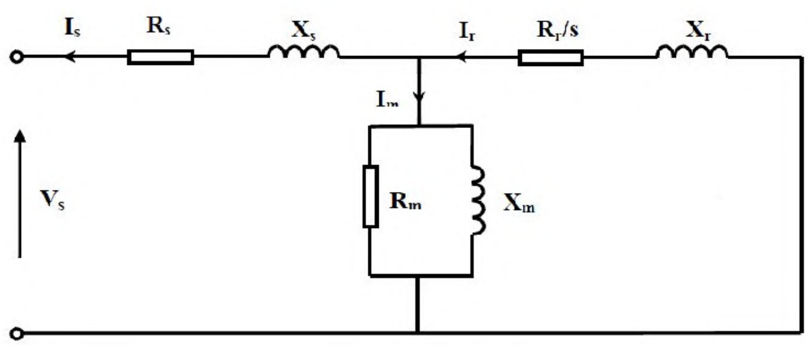

Fig. (3). SFIG Equivalent circuit (Generator convention reference)

The shaft torque of the generator is governed by the following Equation (2):

$$\tau = \frac{3\, V_T^2\, R_2/s}{\omega_s[(R_T + R_2/s)^2 + \ (X_T + X_2)^2]} \tag{4}$$

Thevinin's equivalent circuit parameters; V_T, R_T and X_T, are given by

$$V_T = \frac{V_1 Z_{ms}}{\sqrt{(R_1 + R_{ms})^2 + (X_1 + X_{ms})^2}} \tag{5}$$

$$R_T + \ jX_T = (R_1 + jX_1)//\, jX_m\, //\, R_m \tag{6}$$

Where R_{ms} and X_{ms} are the components of $Z_{ms;}$ the equivalent series impedance of the parallel combination R_m and X_m.

The output current, power factor, active power, reactive power and losses at a specified slip; s and terminal voltage; V_s can be determined as usual for the ac circuit analysis using the generator equivalent circuit.

3.2 Double Fed Induction Generator Modelling

Figure (4) shows a frequency domain circuit model of the 3-phase induction generator when doubly fed [2]. The stator terminal voltage is considered constant assuming an ideal network linking transformer. The injected voltage in the rotor is assumed pure sinusoidal due to the filters action.

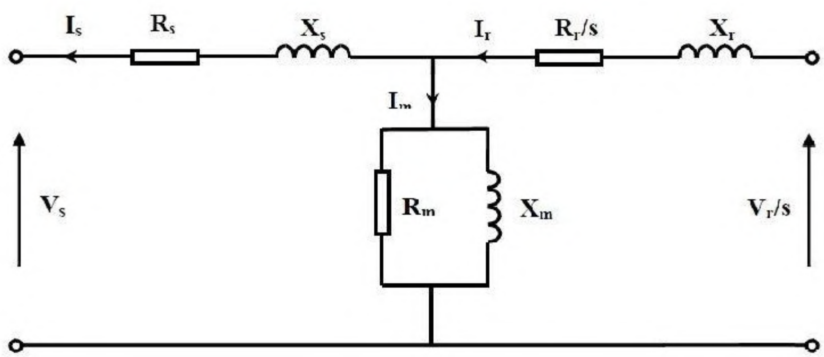

Fig. (4). Equivalent circuit of the DFIG

The equations governing the generator different voltages, currents and power components are as follows:

$P_m = (1\text{-}s)\ (-3\ I_r^2\ R_r/s + 3\ V_r/s\ I_r\ P.f_r)$ (7)

$P_e = 3\ V_s\ I_s\ P.f_s - 3\ V_r\ I_r\ P.f_r$ (8)

$P_{Loss} = P_{core} + P_{cu} = P_m - P_e$ (9)

$\eta = P_e/P_m$ (10)

$Q_s = 3\ V_s\ I_s \sin(\psi_s - \varphi_s)$ (11)

$Q_r = -3\ V_r\ I_r \sin(\psi_r - \varphi_r)$ (12)

In the previous equations, the different phasors are denoted as

$\mathbf{V}_s = V_s \angle \psi_s$, $\mathbf{I}_s = I_s \angle \varphi_s$, $\mathbf{V}_r = V_r \angle \psi_r$ and $\mathbf{I}_r = I_r \angle \varphi_r$ (13)

In the case of the basic control strategy where the rotor injected voltage is in phase or in phase-opposition, the rotor injected voltage can be considered as a voltage drop on a positive or negative resistance added in the rotor circuit.

The induced torque of the induction generator is related to the applied voltage, slip and the equivalent circuit parameters as follows [2]:

$$\tau = \frac{3\ V_T^2\ R_2/s}{\omega_s[(R_T + R_{2t}/s)^2 + (X_T + X_2)^2]} \qquad (20)$$

where V_T, R_T and X_T are the Thevenin's equivalent circuit parameters of the stator, and R_{2t} is the total resistance of the rotor circuit and is given by

$R_{2t} = R_2 + R_{add}$ (21)

Where R_{add} is the virtual added rotor resistance.

$\mathbf{V}_r = -\mathbf{I_r}\ R_{add}$ (22)

Depending on the sign of the added rotor resistance, and adopting the generator convention reference, the rotor injected voltage will be in phase opposition to the rotor current when R_{add} is positive, while it will be in phase with the rotor current when R_{add} is negative.

4. Algorithms and Computation Methodologies

4.1 Algorithm of Computing the Performance of the Single Fed Induction Generator

The SFIG performance characteristics at different wind speeds are determined using the following algorithm:

- i- The generator is assumed to run near its synchronous speed (1500 rpm) at wind speed 6.75 m/s while the tip-speed ratio; λ, at this condition gives the maximum C_p value of the turbine (0.445).
- ii- At other value of the wind speed, keeping in mind that the generator still runs very near to its nominal synchronous speed, the tip-speed ratio is determined.
- iii- Using the characteristic of the wind-turbine (Figure (2)), C_Q and C_p are determined, and consequently the mechanical torque is determined.
- iv- At this torque, the slip is determined using Equation (4).
- v- At this slip, the generator speed is determined, and hence new value of tip-speed ratio is determined. Then the steps are repeated starting from step (iii) till a final value of slip is achieved.
- vi- At this slip, the output current, active power, reactive power and power factor etc. are determined using the equivalent circuit of the SFIG (Figure (3))

4.2 Algorithms of Computing the Performance characteristics of the DFIG

The phase of the rotor injected voltage required to adjust the generator speed and consequently the wind turbine at the point of maximum extracted wind mechanical power depends on the value of the wind speed. At wind speeds higher than the base speed (about 6.75 m/s in our case), the phase is such that electrical power is drawn from the rotor, and the generator is driven at super-synchronous speeds. At wind speeds lower than the base speed, the phase is such that electrical power is delivered to the rotor, and the generator is driven at sub-synchronous speeds. At speeds higher than the base speed, the rotor injected voltage should be in phase opposition with the rotor current or around this phase. At speeds lower than the base speed, the injected rotor voltage should be in phase with the rotor current or around this phase.

An analytical technique is used in the case of the basic control strategy using the following algorithm:

i. At any wind speed, the generator speed and, hence the corresponding generator slip will be determined such that the tip speed ratio is the one corresponding to the maximum power coefficient to trace the maximum extracted wind mechanical power.

ii. At this wind speed, the turbine driving torque corresponding to the maximum extracted wind mechanical power is determined using Figure (2) and Equation (2).

iii. At steady state the induced generator torque is equated to the turbine torque. Thus, using Eqn. 20 is used to determine the virtual added resistance; R_{add} on which the rotor injected voltage appears. Two values of R_{add} will be obtained, and one proper value is chosen such that operation in the stable region is realized.

iv. Using the equivalent circuit of Figure (4) replacing $\mathbf{V_r}$ by R_{add}, all the generator variables such as the stator current, rotor current, output electrical power, losses, efficiency, e.t.c are determined.

5. Results and Discussions

A system consisting of a wind turbine driving a 2 MVA DFIG has been studied. The specifications and parameters of the system are given in Appendix 8.1.

5.1 SFIG Performance Characteristics

To evaluate the performance characteristics of the DFIG, it will be helpful to compare it with the SFIG. The SFIG performance characteristics have been determined using the algorithm given in section 4.1. The initial input tip-speed ratio, torque coefficient, and driving torque at different wind speeds in this case are given in Appendix 8.2.

The computed performance characteristics in case of SFIG are shown in Figures (5-8)

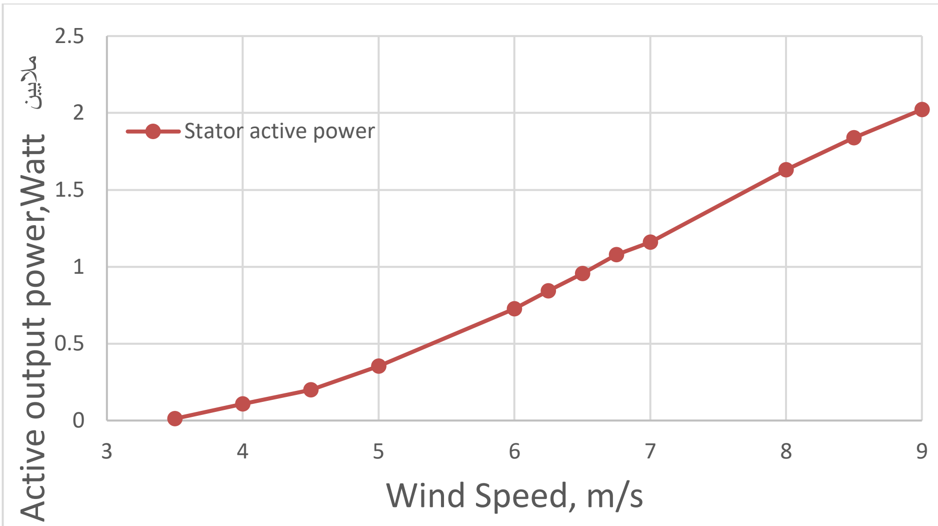

Fig. (5). Output active power in case of SFIG versus the wind speed

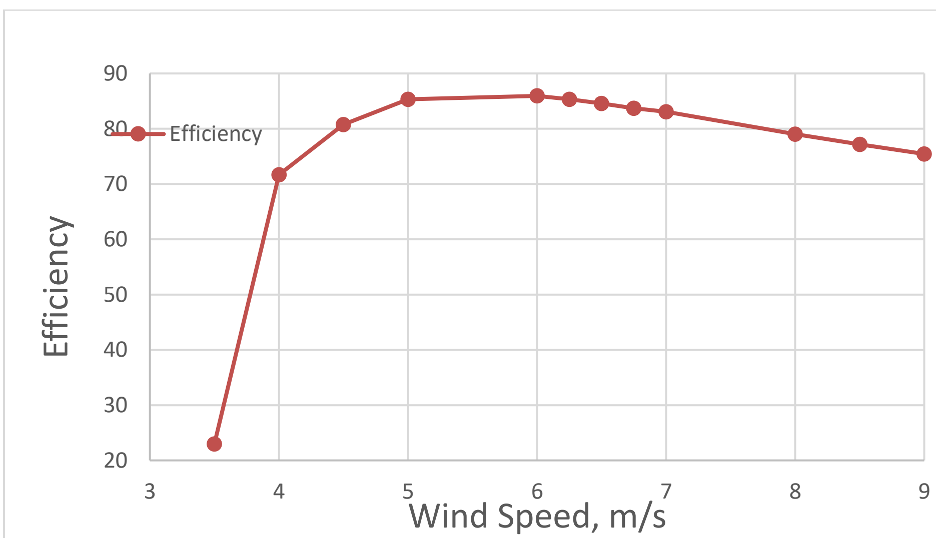

Fig. (6). Generator efficiency versus the wind speed of the SFIG

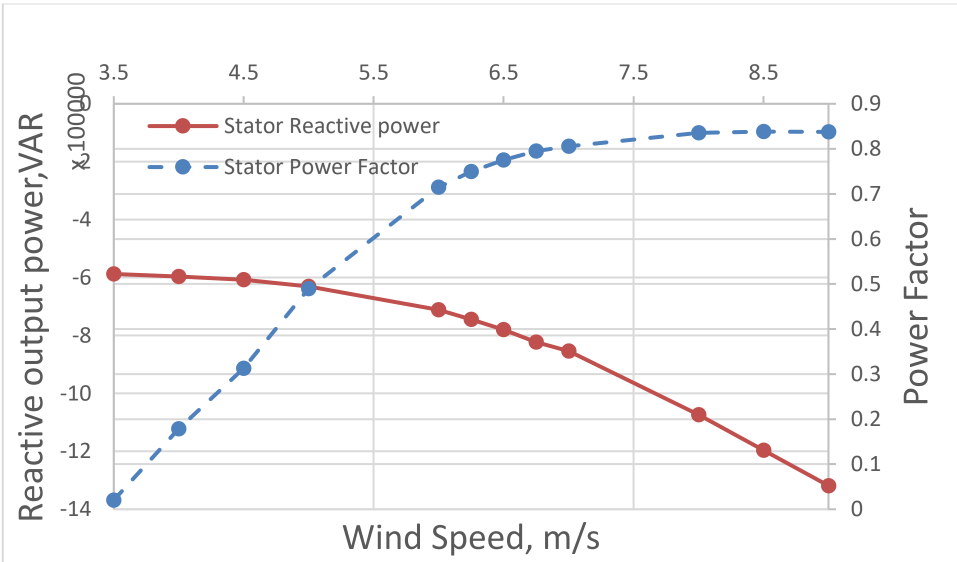

Fig. (7). Output reactive power and power factor of the SFIG versus the wind-speed

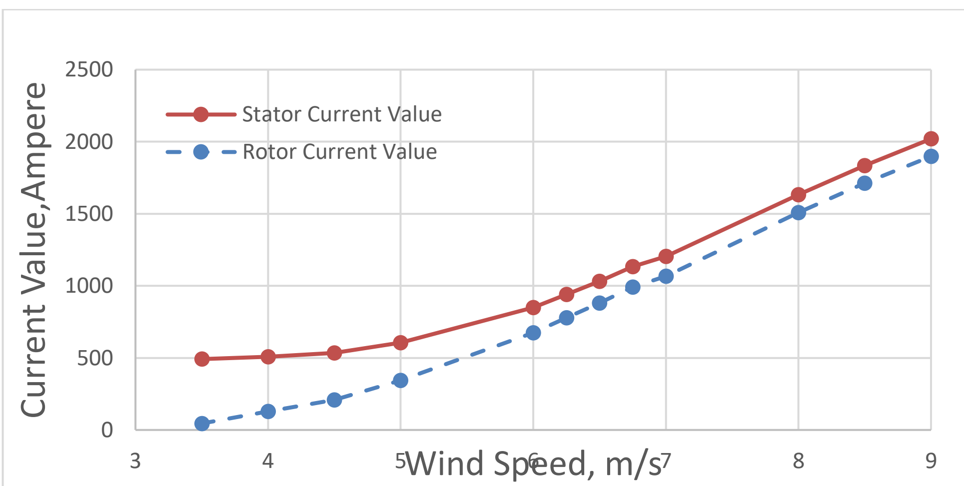

Fig. (8). Stator and rotor currents of the SFIG versus the wind speed

The computed performance characteristics of the SFIG reveals that the output active power increases as the wind speed increases (Figure (5)). The generator efficiency increases as the wind speed increases till it reaches a maximum value of about 86 % at wind speed of about 6 m/s (Figure (6)). At higher wind speeds, the efficiency begins to decrease again. The generator consumes reactive power, and this reactive power increases as the wind speed increases (Figure (7)). Although the reactive power increases with the increase of the wind speed, the stator power factor increases as the wind speed increases. The stator power factor exhibits a saturated pattern at speeds above the base speed (Figure (7)). Investigating the stator and rotor currents depicted in Figure (8), it can be concluded that to avoid overloading the generator, it should not be operated at wind-speed higher than about 8.3 m/s when single-fed. At wind-speeds higher than 8.3 m/s, the stator current will exceed its rated value (1760 A). Thus, the maximum output power is about 1.76 MW at wind speed of 8.3 m/s. It is useless to operate the generator at wind speeds less than 5 as the output power will decrease to the extent that at wind speed around 3.3 m/s, the generated power will not be enough to cover the stator losses. The machine will draw electrical power from the stator side to cover part of the stator losses.

5.2 DFIG Performance Characteristics

The three regions of operation of the DFIG system is shown in Figure (9) which gives the relation between the generator speed and the wind speed over the three regions.

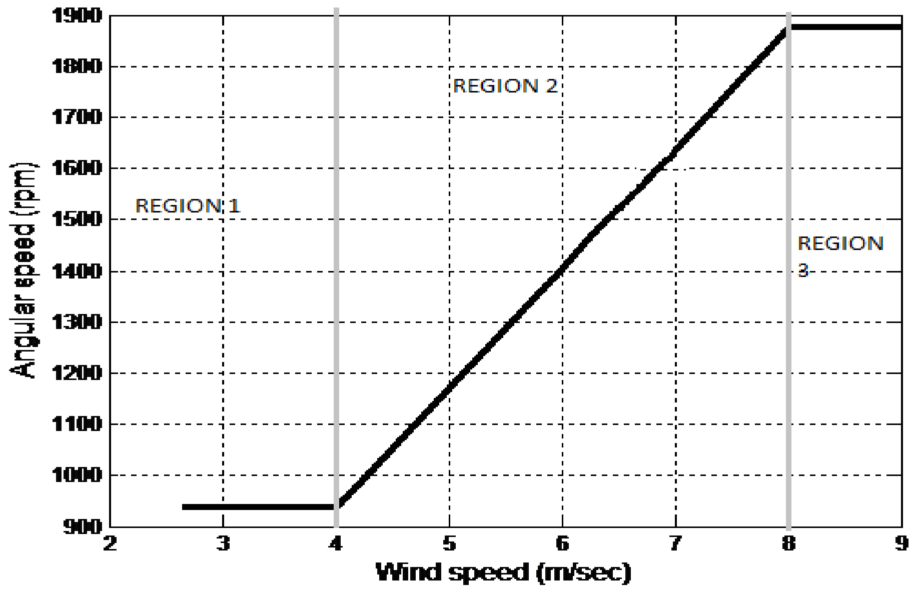

Fig. (9). DFIG speed versus wind speed for the 3-operation regions.

The input mechanical power to the generator at differen wind speeds over the three regions of operation is given in Appendix 8.2.

The magnitudes of the rotor voltage which should be injected in phase or in phase-opposition to the rotor current such that the generator runs at speed enabling the turbine to extract the maximum mechanical power from the wind have been calculated at different wind-speeds using the algorithm presented in Section 4.2. The performance characteristics of the DFIG which is controlled using this basic control algorithm are shown in Figures (10-14).

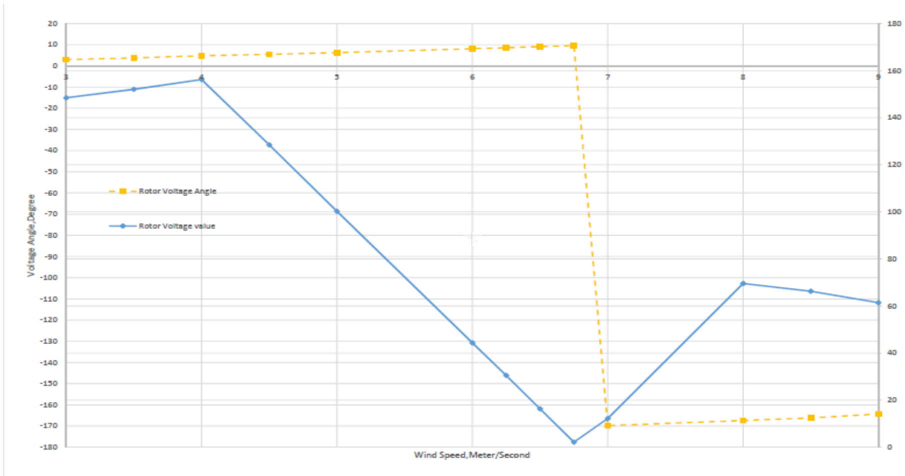

Fig. (10). Magnitude and Phase-angle (w. r. t the stator voltage) of the rotor injected voltage versus the wind speed when employing the basic control strategy

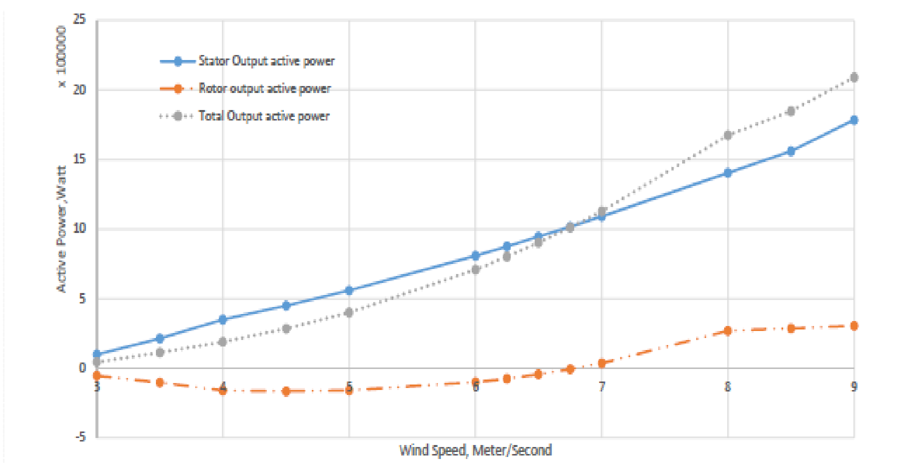

Fig. (11). Stator, rotor and total output active powers versus the wind speed when employing the basic control strategy

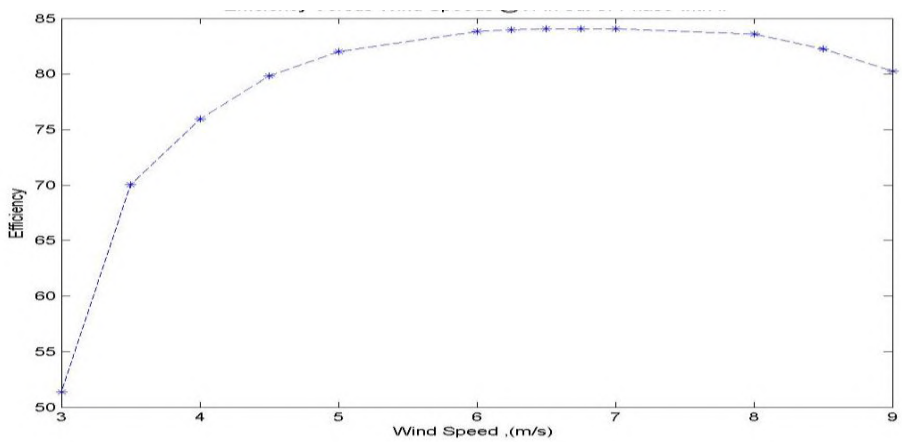

Fig. (12). The generator efficiency versus the wind speed when employing the basic control strategy

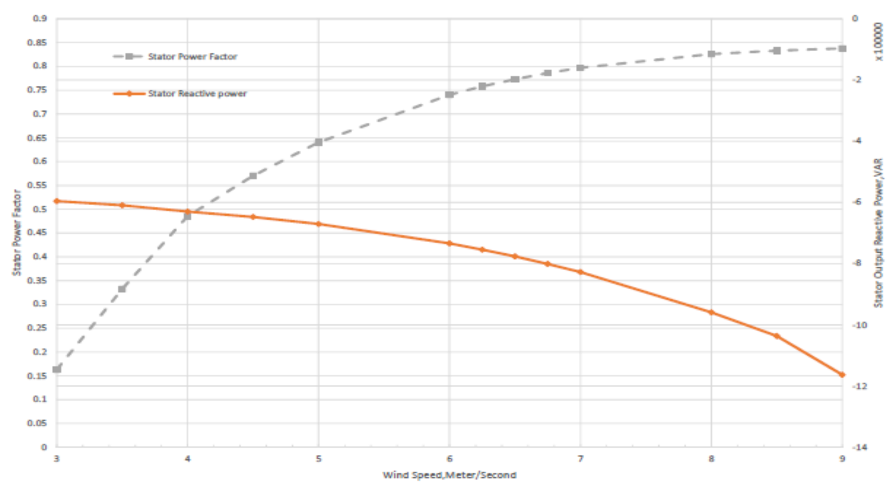

Fig. (13). Stator power factor and output reactive power versus the wind speed when employing the basic control strategy

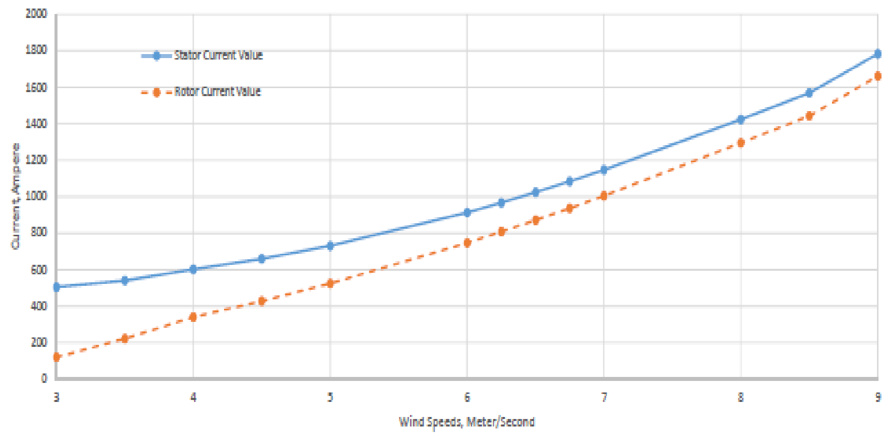

Fig. (14). Stator and rotor currents versus the wind speed when employing the basic control strategy

Comparing the performance characteristics of the DFIG when employing the basic control strategy to those of the SFIG reveals the following:

- The output active power of the generator is increased by double-feeding especially at wind speeds far from the base speed. For example, at wind speed of 3.5 m/s, the total output active power is 0.113645 MW for DFIG while it is about 0.012 MW for SFIG which means an increase of about 847 %. At wind speed of 9 m/s, the total output active power is about 2.09131 MW for DFIG while SFIG is not allowed to work at this speed. The maximum output power of the SFIG is about 1.76 MW at 8.3 m/s. This means an increase of the maximum output power of about 18.82 % (Figures (5 and 11)).
- The generator efficiency has a maximum value of about 84% at wind-speed of about 6.5 m/s, while the lowest efficiency value is about 51.4% at wind speed of 3.0 m/s (Figure (12)).
- The DFIG consumes reactive power from the stator side ranging from 0.59565 MVAR up to 1.16322 MVAR, while the SFIG consumes reactive power ranges

from 0.5876 MVAR at 3.5 m/s up to 1.145 MVAR at 8.3 m/s. The reactive power consumption is more or less the same (Figures (7 and 13)).

- The DFIG does not consume any reactive power from the rotor side. This is expected as the injected voltage is in phase or in phase opposition to the rotor current.
- Although the output power of the generator is clearly increased by doubly feeding it, the stator and rotor currents are almost within their rated values over the entire wind speed range (Figure (14)). The stator current is slightly above its rated value; 1.012 p.u, at wind speed of 9 m/s.

6. Conclusions

The present research is aimed at improving the performance of the double-fed induction generators used with wind turbines at different wind speeds through employing control techniques from the rotor side. The inverter-rectifier set in the rotor circuit has been adjusted to inject a voltage in phase or in phase-opposition to the rotor current such that the generator runs at the speed which allows the wind turbine to extract the maximum mechanical power from the wind, while the apparent power dealt with through the rotor slip rings is minimized.

The results show that the rotor injected voltage phasors required for each control strategy are somewhat different at each wind-speed, and clearly vary as the wind speed changes. The variation can be described for the three modes of operation as follows:

i- Over the first mode of operation and up to the base wind speed, the phase of the rotor injected voltage is around the rotor current phase.

ii- Above the base wind-speed, the phase of the rotor injected voltage is around the phase-opposition of the rotor current.

iii- The magnitude of the rotor injected voltage is more or less constant over the first mode and over the third mode. While, over the second mode it decreases rapidly as the wind speed goes in the direction of the base speed.

The utilized wind energy, and consequently the output power from the DFIG is clearly increased when compared with those of the SFIG.

7. References

[1] Bhim S., "Induction Generators-A prospective", Electrical Machines and Power Systems, Vol. 23, (1995), pp. 163-177.

[2] Akhmatov V., "Induction Generators for Wind Power", Multi-Science Publishing Co. Ltd., Essex, United Kingdom, (2005)

[3] Subbiah V. and Geetha K., "Certain Investigations on a Grid Connected Induction Generator with Voltage Control", Proc. of the IEEE International Conference on Power Electronics, Drives and Energy Systems, New Delhi, India. Jan.(1996), pp. 439-444.

[4] McNerney G., Richardson R. D. and Holly W., "The effect of power electronic converter on power fluctuation and harmonic distortion in a WECS", American society of mechanical engineers, Solar Energy Division, Vol. 9, (1990), pp 237-241.

[5] Suresh S. B., Mariappan G.J. and Palanichamy S., "A Novel Grid Interface for Wind-Driven Grid-Connected Induction Generators", Proc. of IEEE/IAS International Conference on Industrial Automation and Control, Hyderabad, India, Jan.(1995), pp 373-376.

[6] Abdel-halim M. A., "Solid-state control of a grid connected induction generator", Electric Power Components and Systems Journal, Vol. 29, No. 2, (2001), pp. 163-178.

[7] Almarshoud A. F., Abdel-halim M. A., and Alolah A. I., "Control of Grid Connected Induction Generator Using Naturally Commutated AC Voltage Controller", Proc. of IEEE Canadian Conference on Electrical and Computer Engineering (CCECE), Toronto, Canada, May (2001), pp. 839-843.

[8] Almarshoud A. F., Alolah A. I., and Abdel-halim M. A., "Performance of Grid Connected Induction Generator under Naturally Commutated AC Voltage Controller", Electric Power Components and Systems, Vol.32 (7), (2004), pp. 691-700.

[9] Almarshoud A. F., Alolah A. I., and Abdel-halim M. A., "Analysis and Operation of Non-Isolated Three-Phase Induction Generator Controlled by Symmetrical Angle Technique", Proc. of IEE International Conference on Computational Aspects and Their Applications in Electrical Engineering, Jordan, March (2004).

[10] Abdel-halim M. A. and Almarshoud A. F., "Analysis and performance of 3-phase grid-connected induction generator via transistorized ac voltage controller", Transactions on Systems, Signals and Devices, Vol. 3, No. 2, (2007).

[11] Abdel-halim M. A. and Almarshoud A. F., "The Electro-mechanical Performance Characteristics of Network-Connected Induction Generators through Different AC Voltage Controllers, Qassim University Scientific Journal- Engineering and Computer Sciences, Vol. 4, No. 1, (2011).

[12] Carlos R., “Current Control in the Grid Connection of the Double-Output Induction Generator Linked to a Variable Speed Wind Turbine”, Industrial Electronics Conference (IECON), Vol. 2, (2002), pp. 979-984,

[13] Holdsworth L., Wu X. G., Ekanayake J. B., and Jenkins N., “Comparison of Fixed Speed and Doubly-Fed Induction Wind Turbines during Power System Disturbances”, IEE Proceedings Generation, Transmission, and Distribution, Vol. 150, No. 3, pp. 343-352, May (2003).

[14] Fernandez L. M., Garcia C. A., Jurado F., and Saenz J. R., “Aggregation of Doubly Fed Induction Generators Wind Turbines Under Different Incoming Wind Speed”, Proceedings of St. Petersburg Power Tech Conference, St. Petersburg, Russia, June 27-30, (2005).

[15] de Almeidam R. G., and Pecas Lopes J. A., “Primary Frequency Control Participation Provided by Doubly Fed Induction Wind Generators”, Proceedings of the Power System Computation Conference (PSCC), Liege, Belgium, August 22-26, 2005.

[16] Shaltout A. A. and El-Ramahi A. F., "Maximum Power Tracking for a Wind Driven Induction Generator Connected to a Utility Network", Applied Energy, Vol. 52, (1995), pp. 243-253.

[17] Abdel-halim M. A., Mahfouz A. A., and Almarshoud, A. F., "Enhancing the Performance of Wind-Energy-Driven Double-Fed Induction Generators", Qassim University Scientific Journal- Engineering and Computer Sciences, Vol. 7, No. 1, (2014), pp. 23-41.

[18] Bossanyi, E., "The design of closed loop controllers for wind turbines," Wind Energy, Vol. 3 (3), (2000), pp. 149–163.

[19] Leithead, W. and Connor, B., "Control of variable speed wind turbines: design task," International Journal of Control, Vol. 73 (13), (2000), pp. 1189–1212.

8. Appendices

8.1 Generator and Turbine Data

The data and parameters of the studied induction generator and wind-turbine are given in Tables (1-3).

Table (1). Main Characteristics of the Generator

Nominal stator active power	2.0 MW
Nominal torque	12732 Nm
Nominal stator voltage	690 V
Rotor to stator voltage ratio	2.6
Nominal stator current	1760 A
Nominal rotor current referred to the stator side	1807 A
Nominal speed	1500 rpm
Speed range	900–2000 rpm
Pole pairs	2

Table (2). Parameters of the Generator Circuit Model

Magnetizing inductance Lm	2.5 mH
Rotor leakage inductance L_r	0.087 mH
Stator leakage inductance L_s	0.087 mH
Rotor resistance R_r	0.026 ohm
Stator resistance R_s	0.029 ohm

Table (3). Turbine Parameters

Type	Horizontal axis turbine
Radius	62 m
Nominal wind speed	9 m/s
Variable speed ratio (minimum–maximum turbine speed)	9–18 rpm
Optimum tip speed ratio	6.3
Maximum power coefficient C_{p_max}	0.455

8.2 Wind-turbine Initial Mechanical Outputs in Case of SFIG

The wind turbine extracted torques in case of SFIG at different wind speeds are given in Table (4).

Table (4). Initial inputs of the wind-turbine in case of SFIG

Wind-speed, m/s	3	3.5	4	4.5	5	6	6.25	6.5	6.75	7	8	8.5	9
Λ	14.17	12.15	10.61	9.45	8.5	7.08	6.80	6.54	6.3	6.07	5.31	5.00	4.72
C_Q	--	.01152	.02545	.0328	.0441	.0611	.06544	.0688	.07222	.07249	.0800	.081	0.0805
Mechanical torque, Nm	--	330.7	954.1	1556	2583	5154	5989	6810	7710	8323	11996	13712	15278

Appendix 8.3: Wind-turbine Mechanical Power at Different Wind Speeds
The mechanical power extracted from the wind at different wind speeds over the three regions of operation is given in Table (5).

Table (5). Wind-turbine mechanical power at different wind speeds

Wind-speed, m/s	3	3.5	4	4.5	5	6	6.25	6.5	6.75	7	8	8.5	9
Slip	0.375	0.375	0.375	0.2969	0.218	0.062	0.0234	-0.0156	-0.0547	-0.094	-0.25	-0.25	-0.25
Mech. Power	0.0873	0.1623	0.2505	0.35667	0.4893	0.8455	0.9556	1.075	1.20385	1.343	2.0043	2.246	2.6056

التحكم في مولد الحث ثنائي التغذية والمدار بطاقة الرياح لاستخراج أعلى طاقة ميكانيكية

أيمن محمد عبد السميع١ عادل عبد المقصود شلتوت٢

١- قائد فني لفريق المهندسين- شركة نظم الجيزة- القاهرة الجديدة- مصر
٢ - قسم هندسة القوى والآلات الكهربية-كلية الهندسة- جامعة القاهرة- مصر
Aymanabdalsamie@gmail.com

ملخص البحث. استغلال الطاقة المتجددة كطاقة الرياح تجد اهتماما متزايدا هذه الأيام، وتعمل دارة الرياح عند سرعات متغيرة، ولهذا يوصى باستخدام مولد الحث مع تلك الدارة للتوافق مع ذلك . يهدف البحث الحالي إلى تحسين أداء نظام مولد الحث ثنائي التغذية والمدار بطاقة الرياح عند سرعات الريح المختلفة. ولهذا الغرض يستخدام مجموعة مغييرين تربط دائرة العضو الدار بالشبكة وتقوم بحقن جهد معين في دائرة العضو الدوار. هذا الجهد يؤدي إلى دوران المولد عند السرعة التي عندها يستخرج المولد أعلى قدرة ميكانيكية من الرياح. ويقدم البحث طريقة تحليلية جديدة لحساب الجهد المحقون في دائرة العضو الدوار بتمثيله بجهد عبر مقاومة تخيلية موجبة أو سالبة مضافة في الدائرة المكافئة للمولد في نطاق التردد والتي تمثل الحالة المستقرة للمولد. وبناء على نموذج رياضي تم بناؤه طور برنامج حاسوب لحساب خواص أداء المولد، وتم مقارنة الأداء بأداء المولد أحادي التغذية، ولقد أظهرت المقارنة تحسنا ملموسا باستخدام التغذية الثنائية.